Robust Motion Control of Biped Walking Robots

ASHRAF A. ZAHER
Physics Department, Science College
Kuwait University
P. O. Box 5969, Safat 13060
Kuwait
ashraf.zaher@ku.edu.kw

and

MOHAMMED A. ZOHDY
ESE Department - SECS
Oakland University
DHE 137, Rochester, MI 48309
USA
zohdyma@oakland.edu

Abstract: - This paper proposes a robust mathematical approach for motion control. The proposed control technique is applied to a three-degree of freedom Biped walking robot for illustration. The design technique is divided into two major steps; the first one is to establish a robust position control scheme with both guaranteed stability and trajectory tracking capability using a model-reference technique that assumes only the knowledge of the upper bound of the model uncertainty. The performance of this step is investigated for the two cases of point-to-point and trajectory-following motions. The second step is to design an intelligent path planner for the walking Biped that takes all motion constraints into account. Animation is used to check for both motion harmony and trajectory following. The real-time applicability of the proposed controller is investigated and tradeoffs between stability and performance are carefully studied. In addition, real-time potential of the controller is being studied for further application.

Key-Words: - Model-Reference Control, Robotics, GAIT Analysis, and Modeling and Simulation.

1 Introduction

Designing and implementing systems that are capable of controlling unknown plants or adapting to unpredictable changes in the environment have been an active and rich area in control engineering for a long time. Many appealing concepts were proposed in which the notion of Lyapunov functions was often used [1].

Most conventional control techniques are based, either explicitly or implicitly, on a model of the process to be controlled. Problems with control arise when either the system to be controlled is in some way ill defined and/or it is not possible to gain access to the internal variables of the system. Another cause of uncertainty is change of behavior of some system components due to changes in operating conditions, aging, etc. In general, uncertainties can be classified into dynamical due to neglected dynamic components and parametric due imperfect knowledge about one or more of the system components. When access to all system states is available tight feedback control proved to be successful when applied to regulation problems, however for servomechanism the lack of information is much more crucial. In this case, an explicit model can be used to generate estimates of the system's behavior that can be used to modify the closed-loop time response and satisfy the performance specifications [2,3].

In modeling complex systems two forms of complexity can be identified, one given by the amount of detail present in the model of the system, and the other by a lack of information characterizing the relationships between the variables. The former is primarily determined by the degree of accuracy used in developing the model. The lack of information on the relationships between the variables results in uncertain or ill-defined systems. A system is ill defined if its representation is inadequate for the task of control system. The only way to cope with the control of such systems, that are structurally complex, is to transfer the system to a representation with less resolution [4]. Similarly, if the process is ill defined, the system may be represented at a level of abstraction appropriate to the known characteristics of the system. On way to simplify the modeling process is to use multiple models for the same system, based on some scheduling parameter(s). Each model is used to satisfy certain goals or requirements.

Considering robots, including Bipeds, the dynamic models are known to be nonlinear, time-invariant and each link is represented by a second order subsystem [5]. Thus for a robot system having n links a total of $2n$ states, to fully describe the system, are needed. Consequently, the best way to test for stability is by using nonlinear techniques, e.g. phase plane portraits.

Simulations as well as experiments have been conducted by many researchers to investigate the problem of controlling the motion of Biped locomotion [6]. The linear inverted pendulum mode (LIPM), proposed in [7], was successfully applied in practice, where the complexity of the Biped dynamics was reduced via specifying the desired trajectories by a potential energy-conserving orbit. Experimental results using a 12-degree-of-freedom (DOF) walking machine has been reported in [8] that relied on an extended version of this method. The concept of passive dynamic walking, developed in [9], and its energy-based control laws found useful applications for simple unpowered walking machines and both passive and active walking on level ground [10]. In addition, another promising control strategy, based on passive dynamic walking, with the property of automatic GAIT generation was proposed in [11] that realizes dynamics-based control without any approximations such as linearization or disregard of leg mass.

Several control design methodologies for Biped Robots were proposed in the literature. Perhaps, the most common approach was employing tracking of pre-computed reference trajectories that are inspired from biological systems [12], based on simple passive mechanical system that are analogous to Biped robots [9], or calculated through optimization of various cost criteria, such as minimum expended control energy over a walking cycle [13]. A wide range of both model-based and model-free control systems were reported. A continuous time PID controller was used in [14], a robust sliding mode controller was investigated in [15], and a computer-torque controller was established in [16]. Other methods, based on computational intelligence, were also investigated, e.g. [17,18]. In this paper we use a model-reference approach that is capable of accommodating the modeling uncertainties as well motion constraints. This is accomplished via monotonically forcing the errors between the measurable states of the robot and their desired values to zero using a systematic Lyapunov-based method.

Studying the closed-loop stability of nonlinear systems in general, and robotic applications in particular, proved to be a difficult task. Poincaré sections were used in [19], formulating the Biped model as a nonlinear system with impulse effects to simplify the application of the control strategy to under actuated Biped models. Other methods based on Lyapunov direct method and passivity theory were also utilized to investigate the stability of robot systems [20]. In addition, several criteria of stability have been established like ZMP, FRI or HZD [10,21,22]. In this paper, we use a Lyapunov-based approach to establish the stability of the closed-loop system despite the existence of modeling uncertainties.

The rest of this paper is organized such that Sec. 2 introduces the mathematical formulation of the robot dynamics that encapsulates the parameters uncertainty and decomposes the model into two parts, a deterministic and an uncertain. Section 3 investigates generating trajectories for the two cases of point-to-point and human-like motions in 3.1 and 3.2 respectively. The design of the controller is introduced in Sec. 4, and its performance is illustrated in Sec. 5. Section 6 addresses the issue of introducing an intelligent path planner to account for both simple and constrained motions. Finally, a conclusion is given in Sec. 7 summarizing the work done in the paper while proposing future extensions.

2 Modeling of Robots

The robot model takes the form:

$$D(q)\ddot{q} + H(q,\dot{q}) + G(q) = U \tag{1}$$

where

- q is the joint variables (n×1), n is number of joints
- D represents the inertia matrix (n×n)
- H represents the coriolis, centripetal and friction forces (n×1)
- G represents gravitational forces (n×1)
- U represents the input (n×1)

The model has the following uncertainties [23]:

1. Uncertain values for the masses:
   $m_i = m_{i_{nom}}(1+\Delta m_i),\ i = 1, 2, ..., n$
   where *nom.* stands for nominal, Δ represents the uncertainty factor.

2. Viscous and coulomb friction forces inherent in the H matrix:
   $H_{vis} = h_v\dot{q}\ ,\ H_{cou} = h_c\,\mathrm{sgn}(\dot{q})$
   where h_v is diagonal matrix (n×n), h_c is a scalar.

3. Exact value of gravitational acceleration:
   $g = g_{nom}(1+\Delta g)$

resulting in

$$\begin{bmatrix} \dot{X}_{odd} \\ \dot{X}_{even} \end{bmatrix} = \begin{bmatrix} X_{even} \\ D^{-1}(U-H-G) \end{bmatrix}, \text{ or}$$
$$\dot{X} = f(X, U, p) \tag{2}$$

where

X is the state vector
U is the input vector
p is the uncertainty (zero for deterministic systems)

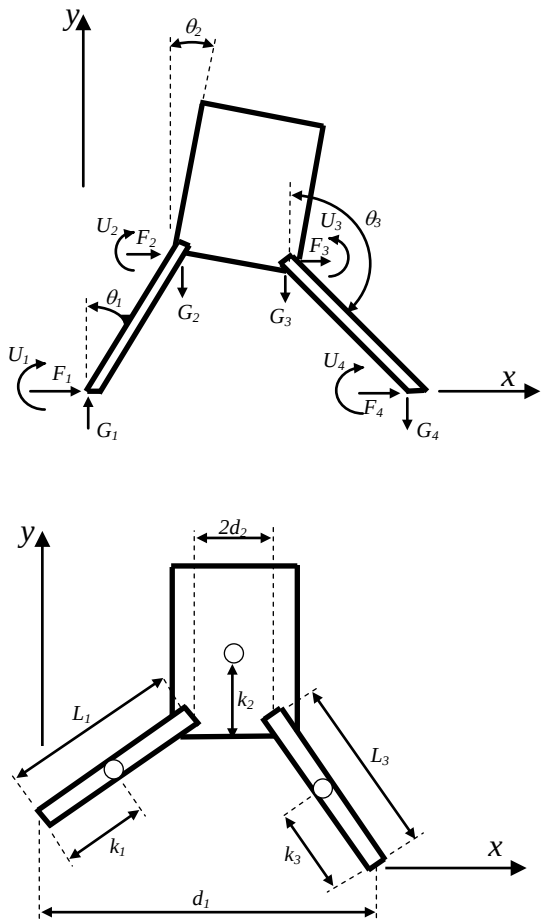

Fig. (1) – Structure of the walking Biped.

Figure (1) shows all the variables and parameters of a walking Biped in the frontal plane that has three degrees of freedom representing two legs (with locked knees, ankles and toes) and the hip [24]. When the Biped is supported by just one leg, either the pair (F_1, G_1) or (F_4, G_4) is equal to zero. In such case, the system can be treated as a three-link planar robot. When either both feet are touching the ground and/or a joint is locked, hard constraints will be encountered. Referring to Fig. (1), two Lagrange multipliers will be needed to fully describe the system, namely the vertical and horizontal ground reactions under the foot.

An explicit model of the walking Biped in the frontal plane can be developed using Newton-Euler method. The same equations can be also obtained using the Lagrangian method and then geometrically projecting the resulting model onto the frontal plane. When both feet are touching the ground, the system is statically indeterminate as there are nine equations in 12 unknowns. This case is easily resolved if u_4, F_4 and G_4 are known. More details can be added to the walking Biped by considering each leg as a new robotic system consisting of three links representing the thigh, shank and foot. This proves to be very useful, especially for animation purposes [25].

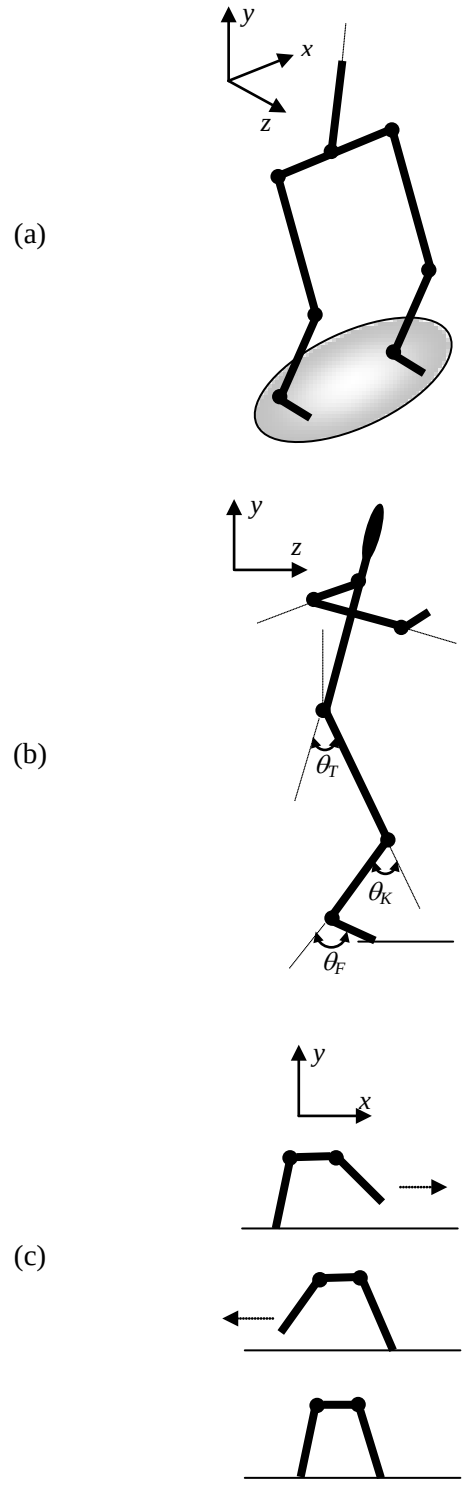

Fig. (2) – The details of the Biped walker in 3D.

Figure (2) shows the structure of the Biped system in the *xyz* space and both *yz* and *xy* planes. As seen from Fig. (2-b) the leg subangles are θ_T, θ_K and θ_F representing the thigh, knee and foot angles respectively. The upper body of the Biped could be included as well as the arm has a similar structure to the leg [26]. The total weight of the body could then by represented as a combination of disturbance forces and torques acting at the connection between the hip and each leg. Magnitude and direction of these disturbances will depend on the nature of motion as well as the surrounding environment.

3 Trajectories (Reference Signals)

When controlling either robots or industrial processes, two main types of control schemes are identified. The first one is regulation for which it is required to force the output into a steady state constant value, usually zero. The second one is servomechanism for which it is required to follow a time-varying signal. It is quite obvious that the later is more complex than the former. Sometimes slowly varying or piecewise reference signals can be dealt with as a regulation problem.

Depending on the environment of the robot system, an optimal choice of reference signals can be made [27]. There are two basic types of trajectories, namely point-to-point motion and coordinated motion.

3.1 Point-to-Point Motion

In choosing the reference model, especially for point-to-point control, the mathematical expression for joint angles should be maximally flat such that initial as well as final values for both the velocity and acceleration signals are zeros. If this was not taken into consideration, the robot system will be forced to follow non-zero initial values for both the velocity and acceleration profiles that might result in too-large control signals that will force the actuators to saturate. Figure (3) shows a typical example for such trajectory that can be calculated using Eq. (3) for the special case $\theta_i = 0$, $\theta_f = 0.3$ rad, and $a = 0.5$, where θ_i and θ_f are the initial and final values of the angle #*j* respectively, and *a* is a time scaling factor.

$$\begin{aligned}\theta_j(t) &= \theta_{jf} - (\theta_{jf} - \theta_{ji})e^{-a_j t^3} \\ \dot{\theta}_j(t) &= 3a_j(\theta_{jf} - \theta_{ji})t^2 e^{-a_j t^3} \\ \ddot{\theta}_j(t) &= 3a_j(\theta_{jf} - \theta_{ji})(2 - 3a_j t^3)te^{-a_j t^3}\end{aligned} \quad (3)$$

where it can be easily verified that all the time derivatives of the angles have both zero initial values and zero final values for $j = 1, 2, \ldots, n$.

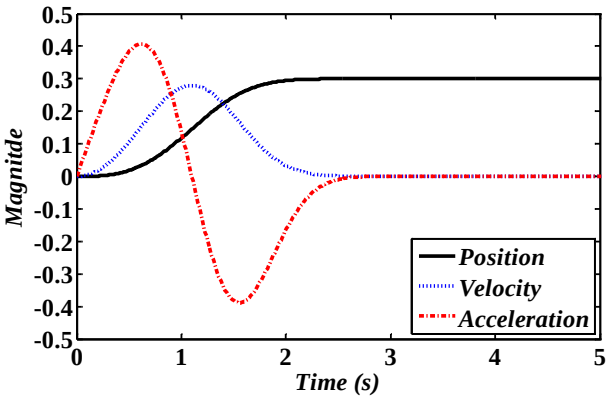

Fig. (3) – Point-to-Point trajectories.

3.2 Coordinated Motion

When performing complicated motions, e.g. walking, it is not sufficient to know just the start and finish point. This is mainly because more than one link will be involved in performing such complex task, hence the trajectories for individual links need to be coordinated to produce a smooth human-like motion. The motion of a human operator during walking is now carefully studied using GAIT analysis [28,29]. A biomechanical model is used to generate the motion trajectory of a typical human leg. Figure (4) represents the data generated from real-time sensors connected to a human operator during an actual walking cycle [30].

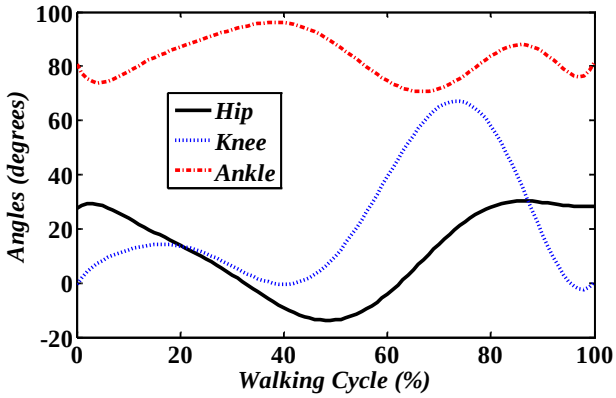

Fig. (4) – A complete walking cycle angles profile.

The trajectories in Fig. (4) are periodic functions; the time necessary to finish one cycle will depend on the actual speed of motion. The values of the angles shown are average values that can be scaled up or down depending on the nature of motion, e.g. walking, jogging or running, and the size of the links as well [31]. On average a complete

walking cycle takes about one second to finish. It was assumed that the contact surface during walking is a smooth horizontal one. The trajectories will be significantly different for irregular surfaces, e.g. inclined, staircase, …, etc.

4 Adaptive Model Reference Control

The design technique is based on constructing an error vector between the robot measurable states and the desired states, then forcing the gradient of this error vector to be negative via the use of a suitable Lyapunov function [32]. The controller is robust in the sense that it accommodates unstructured uncertainties inherent in robotics. This technique is general, i.e. it could be applied to different robots having different degrees of complexities. Introducing a reference linear model in the form:

$$\dot{X}_d = A_d X_d + B_d T_d \tag{4}$$

where

$$A_d = \begin{bmatrix} 0_{n\times n} & I_n \\ -\omega_n^2 I_n & -2\zeta\omega_n I_n \end{bmatrix},$$

$$B_d = \begin{bmatrix} 0_{n\times n} & 0_{n\times n} \\ \omega_n^2 I_n & 0_{n\times n} \end{bmatrix},$$

$$X_d = \begin{bmatrix} X_{d_{odd}} \\ X_{d_{even}} \end{bmatrix},$$

$$T_d = \begin{bmatrix} T_{n\times 1} \\ 0_{n\times 1} \end{bmatrix}$$

gives the following error vector between the desired states of the reference model and the actual states of the robot model:

$$e = X_d - X \tag{5}$$

The error gradient is now given by:

$$\begin{aligned} \nabla e = \dot{e} &= \dot{X}_d - \dot{X} \\ &= (A_d X_d + B_d T_d) - f(X, U, p) \\ &= A_d e + A_d X + B_d T_d - f(X, U, p) \end{aligned}$$

The following quadratic Lyapunov function, V, is now introduced:

$$V(e) = e^T P e$$

where P is a +ve definite symmetric matrix having dimensions $2n\times 2n$ that can be cast in the form:

$$P = \begin{bmatrix} P_{11} & P_{12} \\ P_{21} & P_{22} \end{bmatrix}, \; P_{ij} \text{ has dimension } n\times n,\; i,j = 1,2.$$

Using Eqs. (4) and (5), the following expression is obtained for the gradient of the Lyapunov function:

$$\begin{aligned} \dot{V} &= \dot{e}^T P e + e^T P \dot{e} \\ &= e^T (A_d^T P + P A_d) e \\ &\quad + 2 e^T P (A_d X - f(X, U, p) + B_d T_d) \\ &= -e^T Q e + 2W \end{aligned}$$

From which, it is obvious that sufficient conditions for asymptotic stability of the robot system are given by:

$$A_d^T P + P A_d = -Q, \; Q \text{ is} + \text{ve definite } (2n\times 2n)$$

$$W = 2 e^T P (A_d X - f(X, U, p) + B_d T_d) \le 0$$

If the uncertainties in the robot system are to be considered, it can be assumed that each individual term in Eq. (1) is composed of two terms, a nominal one and an additive perturbation. This can be illustrated as follows:

$$(D_{nom} + \delta D)\ddot{q} + (H_{nom} + \delta H) + (G_{nom} + \delta G) = U$$

from which

$$\begin{aligned} \ddot{q} &= (D_{nom} + \delta D)^{-1}[U - (H_{nom} + \delta H) - (G_{nom} + \delta G)] \\ &= (D_{nom} + \delta D)^{-1}(U - H_{nom} - G_{nom}) \\ &\quad - (D_{nom} + \delta D)^{-1}(\delta H + \delta G) \\ &= D_{nom}^{-1}(U - H_{nom} - G_{nom}) \\ &\quad + D_p(U - H_{nom} - G_{nom}) \\ &\quad - (D_{nom} + \delta D)^{-1}(\delta H + \delta G) \end{aligned}$$

or

$$\ddot{q} = D_{nom}^{-1}(U - H_{nom} - G_{nom}) + \delta f(X, U, p) \tag{6}$$

where

$$\begin{aligned} D_P &= -(D_{nom}\delta D^{-1} D_{nom})^{-1} \\ &= (D_{nom} + \delta D)^{-1} - D_{nom}^{-1} \end{aligned}$$

resulting in:

$$\delta f(X,U,p) = D_p(U - H_{nom} - G_{nom}) - (D+\delta D)^{-1}(\delta H + \delta G)$$

so that the overall uncertain model is represented by:

$$\begin{bmatrix} \dot{X}_{odd} \\ \dot{X}_{even} \end{bmatrix} = \begin{bmatrix} X_{even} \\ D_{nom}^{-1}(U - H_{nom} - G_{nom}) + \delta f(X,U,p) \end{bmatrix} = \begin{bmatrix} X_{even} \\ f_{nom}(X,U,0) + \delta f(X,U,p) \end{bmatrix} \quad (7)$$

Stability analysis using the same Lyapunov function gives:

$$\dot{V} = e^T(A_d^T P + PA_d)e + 2e^T P[A_d X - f_{nom}(X,U,0) - \delta f(X,U,p) + B_d T_d] = -e^T Qe + 2W_p$$

where

$$W_p = e^T P[A_d X - f_{nom}(X,U,0) - \delta f(X,U,p) + B_d T_d]$$
$$W_p \le 0 \quad (8)$$

and

$$\left|\delta f(X,U,p) \le \delta f_{\max}\right| \quad (9)$$

Now Eqs. (8) and (9) are the new design criteria, where U should be found such that the system is asymptotically stable, i.e. $W_p \le 0$. It is assumed that only the upper bound on the uncertainty is known. Moreover, other scenarios for the uncertainty can be accommodated by slightly changing the structure of the design equations.

From Eqs. (6) and (7), we have:

$$\delta f(X,U,p) = -D^{-1}(U - G_{nom} - H_{nom}) + (D+\delta D)^{-1}U - (D+\delta D)^{-1}(H_{nom} + \delta H + G_{nom} + \delta G) = -f_{nom}(X,U,0) + \delta f_1(X,0,p)U + \delta f_2(X,0,p)$$

where

$$\delta f_1(X,0,p) = (D+\delta D)^{-1}$$
$$\delta f_2(X,0,p) = (D+\delta D)^{-1}(H_{nom} + \delta H + G_{nom} + \delta G)$$

Thus Eq. (8) can be written in the form:

$$(e_{odd}P_{12} + e_{even}P_{22})_{1\times n}[-\omega_n^2 I_n X_{odd} - 2\zeta\omega_n I_n X_{even} + \omega_n^2 I_n T_d - \delta f_1(X,0,p)U - \delta f_2(X,0,p)]_{n\times 1} \quad (10)$$

where it is seen that the control signals are direct functions of the proposed second order linear reference model and that they are explicitly expressed as functions of the following parameters:

ω_n: the natural damping frequency
ζ_n: the damping ratio
T_d: the desired torque (computed from the nominal dynamics)
P: the matrix of the design parameters that establishes stability
X_{odd}: measured position signals
X_{even}: measured velocity signals

Thus using Eq. (10) to find a general solution for U is quite difficult due to its dependence on the modeling uncertainty; p, however, the computational complexity can be dramatically reduced by forcing each of the individual n-terms to be negative. The j^{th} term of Eq. (10) has the general form:

$$\left\{\sum_{i=odd}^{2n-1} e_i P_{12_{\frac{i+1}{2},j}} + \sum_{i=even}^{2n} e_i P_{22_{\frac{i}{2},j}}\right\}\left\{\omega_n^2(T_j - x_{2j-1}) - 2\zeta\omega_n x_{2j} - \sum_{k=1}^{n}\hat{D}_{jk}u_k - \delta f_{2_j}\right\} \quad (11)$$

where $\hat{D}_{jk}$, the element in the j^{th} row, and k^{th} column in the matrix $(D+\delta D)^{-1}$, and δf_{2_j}, the j^{th} element in the

$n\times 1$ δf_2 matrix, are the sources of uncertainty.

Assuming that $\left|\delta f_{2j}(X,0,p) \le \delta f_{2j_{\max}}\right|$, Eq. (10) can be further manipulated to take the form:

$$(D+\delta D)^{-1}U = \begin{bmatrix} \omega_n^2(T_1 - x_1) - 2\zeta\omega_n x_2 - \text{sgn}\left\{\sum_{i=odd}^{2n-1} e_i P_{12_{\frac{i+1}{2},1}} + \sum_{i=even}^{2n} e_i P_{22_{\frac{i}{2},1}}\right\}\delta f_{2_{1\max}} \\ \omega_n^2(T_2 - x_3) - 2\zeta\omega_n x_4 - \text{sgn}\left\{\sum_{i=odd}^{2n-1} e_i P_{12_{\frac{i+1}{2},2}} + \sum_{i=even}^{2n} e_i P_{22_{\frac{i}{2},2}}\right\}\delta f_{2_{2\max}} \\ \vdots \\ \omega_n^2(T_n - x_{2n-1}) - 2\zeta\omega_n x_{2n} - \text{sgn}\left\{\sum_{i=odd}^{2n-1} e_i P_{12_{\frac{i+1}{2},n}} + \sum_{i=even}^{2n} e_i P_{22_{\frac{i}{2},n}}\right\}\delta f_{2_{n\max}} \end{bmatrix}$$

Finally, assuming that $\left|\delta D\right| \le \delta D_{\max}$, U is given by:

$$u_j = \left\{\sum_{i=1}^{n} D_{ji} + n\delta D_{j_{\max}}\,\text{sgn}\left[f_j(e)\right]\right\}\left\{\omega_n^2(T_j - x_{2j-1}) - 2\zeta\omega_n x_{2j} - \text{sgn}\left[f_j(e)\right]\delta f_{2_{j_{\max}}}\right\} \tag{12}$$

where

$$f_j(e) = \sum_{i=odd}^{2n-1} e_i P_{12_{\frac{i+1}{2},j}} + \sum_{i=even}^{2n} e_i P_{22_{\frac{i}{2},j}}\text{, and } \delta D_{j_{\max}} = \max(D_{ji}), i = 1,2,...n$$

The control law, given by Eq. (12), is a function of only the available information about the system uncertainty, and guarantees a stable performance, thus the controller design is robust. The controller can be implemented in an incremental mode for small perturbation in the system [33]. The response of the system is indeed satisfactory as indicated in Fig. (5) for the case ω_n = 8 rad/s and ζ = 1.

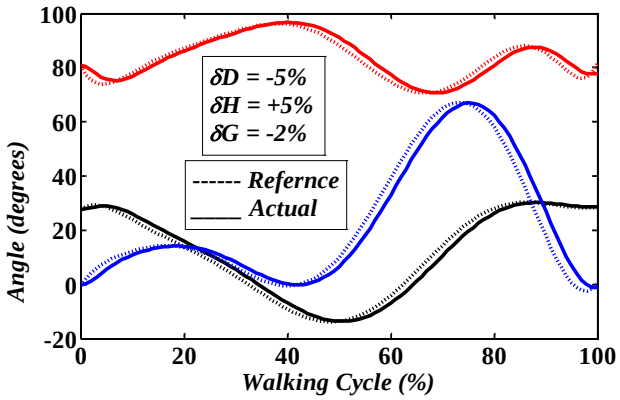

Fig. (5) – A complete walking cycle angles profile.

Fig. (6) shows a three-dimensional uncertainty configuration for the perturbed robot system, where the operating condition could be anywhere in the parallelogram. The point at (0.5, 0, 9.81) represents the condition of the nominal mode. It is quite evident that as the number of links increases the dimensions of the perturbation space increase.

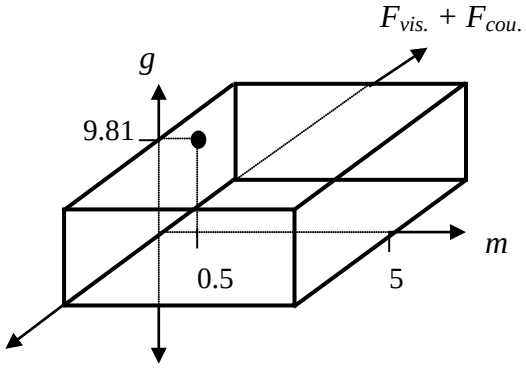

Fig. (6) – A three dimensional perturbation space for the robot system.

5 Response Analysis

Fig. (7) shows the response of the proposed controller for a complete motion cycle. The coupling from each leg to the other is treated as a disturbance that

its effect can be neglected due the function of the upper portion of the human body that counter-balances the weight of the body during motion. The motion of each leg is 50% out of phase with each other. It was assumed that the robot is moving along a horizontal plane and that the motion was not constrained. Thus, with reference to Figs. (1) and (2), the entire walking robot can be thought of as a seven degrees-of-freedom system, three for each leg and the hip. During walking, each leg is represented by a planar three degrees-of-freedom system, with the net effect of the coupling caused by the other leg, the hip and the upper body equal to zero.

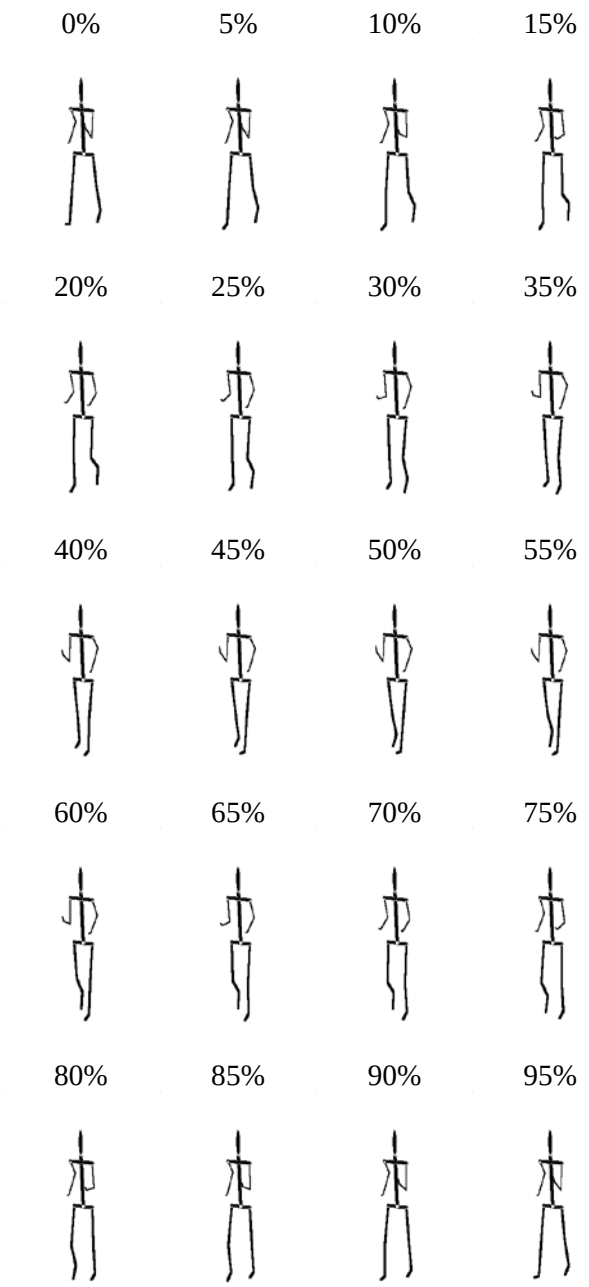

Fig. (7) – Snap Shots of Motion.

A path planner can be designed to generate the required profile for the motion angles that will be used as dynamic set points for the individual links. Animation was used to check for the harmony of motion and that the sub-angles are coordinated according to the GAIT profiles.

5.1 Constrained Motion

Constraints may be introduced into the state space representation of the system, so that the actual motion may be temporarily restricted to a smaller, completely controllable subspace of the original state space. The original state space need to be preserved for conceptual and computational reasons as the reduced subspace has no natural coordinate system and may also vary with time. During calculations (simulations), it is possible to associate with each constraint a corresponding constraint force that can be used as a control to maintain or deliberately violate the constraint being studied [24].

Two types of constraints need to be identified, those that are deliberately imposed or violated by the designer; e.g. maintaining a double support stance for the Biped, and those that are randomly imposed by the environment; e.g. accidentally colliding with a rock causing the foot to be immediately immobilized. The difficulty of representing the constraints will also depend on whether collisions or contacts have elastic or plastic nature. Lagrangian dynamics will be used to construct a new model for the Biped system subject to the following constraints:

1. The Biped is supported by on one leg and the movement of the system is constrained so that the second foot is maintained at ground level but is permitted to move horizontally without touching the ground.
2. Both feet of the Biped are on the ground and the Biped is swaying to either left or right such that the weight of the system is gradually transferred to either legs.

Introducing the kinetic energy; *K.E.*, potential energy; *P.E.*, generalized inertia; $I(\Theta)$, constraints; C, exogenous inputs U, constraint forces; F_C and the Lagrange operator; L, the following equations can be obtained:

$$\frac{d}{dt}\left(\frac{\partial L}{\partial \dot{\Theta}}\right)-\left(\frac{\partial L}{\partial \Theta}\right)=\left(\frac{\partial C}{\partial \Theta}\right)^{T} F_C + U$$

From which, we have:

$$I(\Theta)\ddot{\Theta}+H(\Theta,\dot{\Theta})+G(\Theta)=\left(\frac{\partial C}{\partial \Theta}\right)^{T} F_C + U$$

Solving for the states, angles and angular velocities, we get:

$$\ddot{\Theta} = I(\Theta)^{-1}\left[U - H(\Theta,\dot{\Theta}) - G(\Theta) + \left(\frac{\partial C}{\partial \Theta}\right)^T F_C\right] \quad (13)$$

where

$$L = K.E. - P.E.$$
$$K.E. = \frac{1}{2}\dot{\Theta}^T I(\Theta)\dot{\Theta}$$
$$P.E. = P.E.(\Theta)$$
$$C(\Theta) = 0$$
$$U = \begin{bmatrix} u_1 & u_2 & u_3 \end{bmatrix}^T$$
$$F_C = \begin{bmatrix} G_1 & F_1 \end{bmatrix}^T \text{ or } \begin{bmatrix} G_4 & F_4 \end{bmatrix}^T$$

and

$$\Theta = \begin{bmatrix} \theta_1 & \theta_2 & \theta_3 \end{bmatrix}^T$$
$$\dot{\Theta} = \begin{bmatrix} \dot{\theta}_1 & \dot{\theta}_2 & \dot{\theta}_3 \end{bmatrix}^T$$

Now, Eq. (9) can be cast in the form:

$$\dot{X} = f(X, U, F_C) \quad (14)$$

where

$$X = \begin{bmatrix} \theta_1 & \dot{\theta}_1 & \theta_2 & \dot{\theta}_2 & \theta_3 & \dot{\theta}_3 \end{bmatrix}^T$$
$$\dot{X} = \begin{bmatrix} \dot{\theta}_1 & \ddot{\theta}_1 & \dot{\theta}_2 & \ddot{\theta}_2 & \dot{\theta}_3 & \ddot{\theta}_3 \end{bmatrix}^T$$

Twice differentiating the constraints equation, we arrive at the following:

$$\frac{\partial^2 C}{\partial t^2} = \overline{C}(X)\dot{X} = 0 \quad (15)$$

Thus, from Eqs. (10) and (11) we arrive at:

$$\overline{C}(X) f(X, U, F_C) = 0 \quad (16)$$

Now Eq. (16) provides the necessary equations to solve for the unknown constraint forces. Manipulating Eq. (16) results in:

$$\left[\frac{\partial}{\partial \Theta}\left(\frac{\partial C}{\partial \Theta}\right)\dot{\Theta}\right]\dot{\Theta} + \frac{\partial C}{\partial \Theta} I^{-1}(\Theta)\left[H(\Theta,\dot{\Theta}) + G(\Theta) - U\right] = \left[\frac{\partial C}{\partial \Theta} I^{-1}(\Theta)\frac{\partial C^T}{\partial \Theta}\right] F_C$$

or

$$F_C = \left[\frac{\partial C}{\partial \Theta} I^{-1}(\Theta)\frac{\partial C^T}{\partial \Theta}\right]^{-1}\left\{\left[\frac{\partial}{\partial \Theta}\left(\frac{\partial C}{\partial \Theta}\right)\dot{\Theta}\right]\dot{\Theta} + \frac{\partial C}{\partial \Theta} I^{-1}(\Theta)\left[H(\Theta,\dot{\Theta}) + G(\Theta) - U\right]\right\} \quad (17)$$

Now, using Eq. (17), F_C can be expressed as a function of the states and the inputs resulting in:

$$\dot{X} = f(X, U, F_C(X,U)) = f(X,U) \quad (18)$$

Thus Eq. (18) can be solved directly for the system states.

5.2 Examples of Constrained Motion

Two different cases will be investigated to show the constraints effect on the motion, the first one is simple and the second one is rather complicated [24]. In both cases, Fig. (1) was used in the analysis and Figs (8) and (9) illustrate the details.

5.2.1 Case I: sliding foot

$$C_1 \Rightarrow F_1 = G_1 = u_1 = 0 \text{ and } C_2 \Rightarrow \theta_2 = \dot{\theta}_2 = 0$$

Thus,

$$F_C = 0 \Rightarrow \begin{bmatrix} 0 & 0 & 1 & 0 & 0 & 0 \\ 0 & 0 & 0 & 1 & 0 & 0 \end{bmatrix} X = 0$$

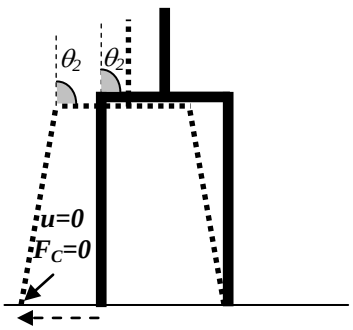

Fig. (8) – Constrained motion (case I).

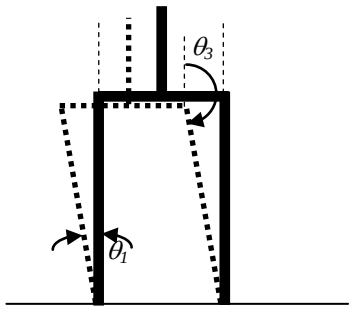

Fig. (9) – Constrained motion (case II).

5.2.2 Case II: sway motion

$$C_1 \Rightarrow L\cos\theta_1 - 2d_2\sin\theta_2 + L_3\cos\theta_3 = 0$$

and

$$C_2 \Rightarrow L_1\sin\theta_1 + 2d_2\cos\theta_2 + L_3\sin\theta_3 - d_1 = 0$$

thus,

$$\frac{\partial C_1}{\partial t} = -L_1\dot{\theta}_1\sin\theta_1 - 2d_2\dot{\theta}_2\cos\theta_2 - L_3\dot{\theta}_3\sin\theta_3$$

$$\frac{\partial C_2}{\partial t} = L_1\dot{\theta}_1\cos\theta_1 - 2d_2\dot{\theta}_2\sin\theta_2 + L_3\dot{\theta}_3\cos\theta_3$$

$$\frac{\partial^2 C_1}{\partial t^2} = -L_1\ddot{\theta}_1\sin\dot{\theta}_1 - L_1\dot{\theta}_1^2\cos\theta_1 - 2d_2\ddot{\theta}_2\cos\theta_2 + 2d_2\dot{\theta}_2^2\sin\theta_2 - L_3\ddot{\theta}_3\sin\theta_3 - L_3\dot{\theta}_3^2\cos\theta_3$$

$$\frac{\partial^2 C_2}{\partial t^2} = L_1\ddot{\theta}_1\cos\dot{\theta}_1 - L_1\dot{\theta}_1^2\sin\theta_1 - 2d_2\ddot{\theta}_2\sin\theta_2 - 2d_2\dot{\theta}_2^2\cos\theta_2 + L_3\ddot{\theta}_3\cos\theta_3 - L_3\dot{\theta}_3^2\sin\theta_3$$

Now, using Eq. (11), the constraints can be represented by:

$$\begin{bmatrix} \frac{\partial^2 C_1}{\partial t^2} \\ \frac{\partial^2 C_2}{\partial t^2} \end{bmatrix} = \begin{bmatrix} -L_1x_2\cos x_1 & -L_1\sin x_1 & 2d_2x_4\sin x_3 & -2d_2\cos x_3 & -L_3x_6\cos x_5 & -L_3\sin x_5 \\ -L_1x_2\sin x_1 & L_1\cos x_1 & -2d_2x_4\cos x_3 & -2d_2\sin x_3 & -L_3x_6\sin x_5 & L_3\cos x_5 \end{bmatrix}\dot{X}$$

For the special case when both feet are parallel and motion is considered near the vertical, these constraints reduce to:

$$d_1 = 2d_2 \Rightarrow \begin{cases} \theta_3 - \theta_1 = \pi \\ \dot{\theta}_3 - \dot{\theta}_1 = 0 \end{cases}$$

or in a state space form:

$$\begin{bmatrix} 1 & 0 & 0 & 0 & -1 & 0 \\ 0 & 1 & 0 & 0 & 0 & -1 \end{bmatrix} X = \begin{bmatrix} \pi \\ 0 \end{bmatrix}$$

6 Coordinated Motion (Path Planner)

In order for the robot to accomplish a smooth walking motion, it will be necessary to coordinate the motion of at least seven degrees-of-freedom as depicted in Figs. (1) and (2). The motion analysis can be dramatically simplified when considering planar motion rather than motion in three-dimensional space. During normal walking scenarios, both legs will exhibit the same type of motion, while moving in two parallel planes, except for a phase difference that is equal to 50% of the overall 100% walking cycle. Also, during walking the coupling or interacting between both legs is compensated for by the counter-balance motion of both the hip and upper portion of the human body. The trajectory of motion given by Fig. (4) represent only the average measurements of angles during a complete walking cycle on a level surface. These angles can differ in value depending on the speed of motion and the structure of the human body, e.g. how tall the walking (Biped) person is. In addition, walking up a hill or going up the stairs will change the angle profile. Also locking one or more of the joints or imposing any additional constraints will result in deforming the default angles profile.

Thus an intelligent path planner is required to provide a coordinated smooth motion by generating the best profile for the link angles and their time derivatives that takes care of constraints imposed by either the surrounding environment or the physical structure of the walking Biped. Fig. (10) shows a flow chart illustration of the complete process of path planning and control.

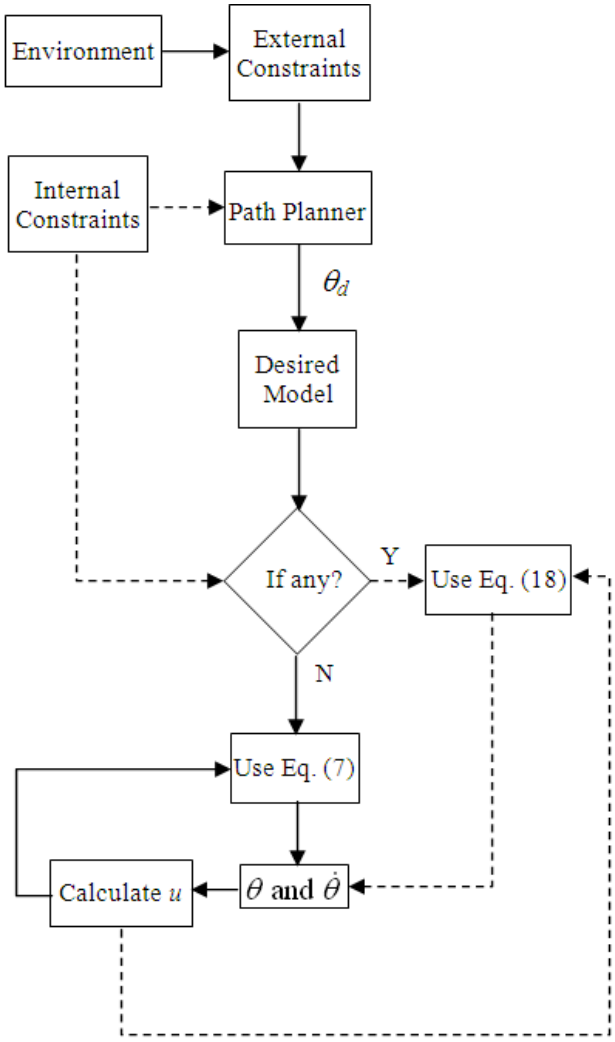

Fig. (10) – The complete system.

7 Conclusion

In order to design robust controllers for robots, the model uncertainties must be considered. One way to do this is by expressing the mathematical model in such a way that will encapsulate both the nominal behavior as well as modeling uncertainty. For unperturbed (normal) operating conditions, the terms corresponding to uncertainties are simply cancelled. However, the information about the upper bounds of the uncertainties must be known in advance. Solving for the control law, for the perturbed case, will involve the uncertainty term and it will be difficult to calculate *U*, especially for increasing number of links. A unique solution is usually unavailable, as a family of solutions will exist, from which we have to choose the simplest causal one. Although, for the proposed control law, the robot system stability was assured, more effort must be done to have a satisfactory performance. This can be done by properly choosing the *Q* matrix and/or the structure of the reference model. The control signal was a function of the error signal and its derivative, i.e. the controller is of *PD* nature. Thus the system might suffer steady state errors even when it is stable and having satisfactory response. One possible solution is to implement the controller in an incremental form to add an integral action to it and, hence, removing any offsets. Although we chose a rather simple Lyapunov function for our analysis and design of the control law, more suitable forms could be tried. A rather promising one is *V(X,U) = K.E. + P.E.*, accounting for both the kinetic and potential energies of the robot system respectively. The simulation as well as the animation, carried out in this paper, proved that the proposed controller will always have a satisfactory and stable performance for both regulation and servomechanism applications.

It should be emphasized that although a Biped robot system was chosen to exemplify the application of the proposed controller to a complex nonlinear system, it can be successfully applied to other nonlinear applications as well [34,35]. All what is necessary to accommodate a different system is to carefully choose the reference model such that the control effort is achievable to avoid adding unnecessary nonlinearities due to saturation that might cause the closed-loop system to become uncontrollable and/or unstabilizable. In addition, the choice of the Lyapunov function can be a bottleneck in the design process; but for most systems a simple quadratic form will be adequate and will systemize the analysis and design of the proposed controller.

References:

[1] M. Krstic, I. Kanellakopoulus and P. Kokotovic, *Nonlinear and Adaptive Control Design*, John Wiley & Sons Inc., 1995.

[2] J. J. E. Slotine and W. Li, *Applied Nonlinear Control*, Prentice Hall, 1991.

[3] H. Khalil, *Nonlinear Systems*, Prentice Hall, 3rd Edition, 2002.

[4] S. Petterson and B. Lennarston, Stability and Robustness of Hybrid Systems, *Proceedings of the 35th IEEE Conference on Decision and Control*, Kobe, Japan, 1996, pp. 1202-1207.

[5] H. Asada, *Robot Analysis and Control*, John Wiley, NY, 1986.

[6] F. Asano, M. Yamakita, N. Kamamichi, L. Zhi-Wei, A novel gait generation for biped walking robots based on mechanical energy constraint, *IEEE Transactions on Robotics and Automation*, Vol. 20, No. 3, 2004, pp. 565-573.

[7] S. Kajita, T. Yamaura, and A. Kobayashi, Dynamic walking control of a biped robot along a potential conserving orbit, *IEEE Transactions on Robotics and Automation*, Vol. 8, 1992, pp. 431-438.

[8] S. Kajita, O. Matsumoto, and M. Saigo, Real-time 3-D walking pattern generation for a biped robot with telescopic legs, *Proceedings of the IEEE International Conference of Robotics and Automation*, 2001, pp. 2299-2306.

[9] T. McGeer, Passive Dynamic Walking, *International Journal of Robotics Research*, Vol. 9, No. 2, 1990, pp. 62-82.

[10] M. Goswami, B. Espiau, and A. Keramane, Limit Cycles in a Passive Compass Gait Biped and Passivity-Mimicking Control Laws, *Autonomous Robots*, Vol. 4, No. 3, 1997, pp. 273-286.

[11] M. W. Spong, Passivity-based control of the compass gait biped, *Proceedings of the World Congress IFAC*, 1999, pp. 19-23.

[12] M. Vukobratovic, B. Borovac, D. Surla, and D. Stokic, *Biped Locomotion*, Springer-Verlag, 1990.

[13] M. Rostami and G. Bessonnet, Impactless sagittal gait of a biped robot during the single support phase, *Proceedings of the IEEE International Conference on Robotics and Automation*, Leuven, Belgium, 1998, pp. 1385-1391.

[14] J. Furusho and A. Sano, Sensor-based control of a nine-link biped, *International Journal of Robotics Research*, Vol. 9, No. 2, 1990, pp. 83-98.

[15] S. G. Tzafestas, A. E. Krikochoritis, and C.S. Tzafestas, Robust Sliding-mode Control of Nine-link Biped Robot Walking, *Journal of Intelligent and Robotic Systems*, Vol. 20, No. 2-4, 1997, pp. 375-402.

[16] N. Chaillet, G. Abba, and E. Ostertag, Double dynamic modeling and computed-torque control of a biped robot, *Proceedings of the IEEE/RSJ International Conference on Intelligent Robotics Systems*, Munich, Germany, 1994, pp.1149-1153.

[17] J.-G. Juang, Intelligent Trajectory Control using Recurrent Averaging Learning, *Applied Artificial Intelligence*, Vol. 15, No. 3, 2001, pp. 277-296.

[18] B. L. Luk, S. Galt, and S. Chen, Using genetic algorithms to establish efficient walking gaits for an eight-legged robot, *International Journal of Systems Science*, Vol. 32, No. 6, 2001, pp. 703-713.

[19] J. W. Grizzle, G. Abba, and F. Plestan, Asymptotically stable walking for biped robots: Analysis via systems with impulse effects, *IEEE Transactions on Automatic Control*, Vol. 46, No. 1, 2001, pp. 51-64.

[20] Y. Hurmuzlu, F. Génotb, and B. Brogliato, Modeling, stability and control of biped robots – a general framework, *Automatica*, Vol. 40, No. 10, 2004, pp. 1647-1664.

[21] A. Goswami, Postural stability of biped robots and the foot-rotation indicator (fri) point, International *Journal of Robotics Research*, Vol. 18, No. 6, 1999, pp. 523-533.

[22] J. W. Grizzle, C. Chevallereau, C. C.-L. Shih, HZD-based control of a five-link under actuated 3D bipedal robot, *Proceedings of the 47th IEEE Conference on Decision and Control*, Cancun, Mexico, 2008, pp. 5206-5213.

[23] M. Zohdy and A. Zaher, Robust Control of Biped Robots, *Proceedings of the American Control Conference*, Chicago, IL, USA, 2000, pp. 1473-1477.

[24] H. Hemami and B. Wyman, Modeling and Control of Constrained Dynamic Systems with Applications to Biped Locomotion in the frontal plane, *IEEE Transactions on Automatic Control*, Vol. 24, No. 4, 1997, pp. 526-535.

[25] A. Zaher and M. Zohdy, Real-Time Model-Reference Control of Nonlinear Processes, *Proceedings of the 2nd International Conference on Computing and Information*, Manama, Bahrain, 2000, pp. 35-42.

[26] M. Wisse, A. L. Schwab, and F. C. T. van der Helm, Passive dynamic walking model with upper body, *Robotica*, Vol. 22, No. 6, 2004, pp. 681-688.

[27] Q. Huang, K. Yokoi, S. Kajita, K. Kaneko, H. Arai, N. Koyachi, and K. Tanie, Planning Walking Patterns for a Biped Robot, *IEEE Transactions on Robotics and Automation*, Vol. 17, No. 3, 2001, pp. 280-289.

[28] R. L. Criak and C. A. Oatis, *GAIT Analysis: Theory and Application*, St. Louis: Mosby, c1995.

[29] A. Marlene, *Biomechanics of Human Movements*, Madison, Wis.: Brown & Benchmark, c1995.

[30] A. Dasgupta and Y. Nakamura, Making Feasible Walking Motion of Humanoid Robots From Human Motion Capture Data, *Proceedings of the IEEE International Conference on Robotics and Automation*, Detroit, Michigan, 1999, pp. 1044-1049.

[31] Y.-L. Chen, Y.-c. Li, T.-S. Kuo, and J.-S. Lai, The development of a closed-loop controlled functional electrical stimulation (FES) in gait training, *Journal of Medical Engineering and Technology*, Vol. 25, No. 2, 2001, pp. 41-48.

[32] A. Datta and P. A. Iaonnou, Performance Analysis and Improvements in Model Reference Adaptive Control, *IEEE Transactions on Automatic Control*, Vol. 39, 1994, pp. 2370-2387.

[33] A. Zaher and M. Zohdy, Robust Model Reference Control for a Class of Nonlinear and Piecewise Linear Systems, *Proceedings of the American Control Conference*, Vol. 6, Arlington, VA, USA, 2001, pp. 4514-4519.

[34] A. Zaher and A. Abu-Rezq, Adaptive model-reference control for a class of uncertain nonlinear systems using a simple systematic Lyapunov-based design, *Journal of Circuits, Systems, and Computers*, Vol. 17, No. 4, 2008, pp. 539-559.

[35] A. Harb and A. Zaher, Nonlinear Control of Permanent Magnet Stepper Motors, *Journal of Nonlinear Science and Numerical Simulation*, Vol. 9, No. 4, 2004, pp. 443-458.